NANO LETTERS

Letter

pubs.acs.org/NanoLett

Gate-Tunable Electron Transport Phenomena in Al–Ge⟨111⟩–Al Nanowire Heterostructures

Florian M. Brunbauer, Emmerich Bertagnolli, and Alois Lugstein*

Institute for Solid State Electronics, Technische Universität Wien, Floragasse 7, 1040 Vienna, Austria

Supporting Information

ABSTRACT: Electrostatically tunable negative differential resistance (NDR) is demonstrated in monolithic metal–semiconductor–metal (Al–Ge–Al) nanowire (NW) heterostructures integrated in back-gated field-effect transistors (FETs). Unambiguous signatures of NDR even at room temperature are attributed to intervalley electron transfer. At yet higher electric fields, impact ionization leads to an exponential increase of the current in the ⟨111⟩ oriented Ge NW segments. Modulation of the transfer rates, manifested as a large tunability of the peak-to-valley ratio (PVR) and the onset of impact ionization is achieved by the combined influences of electrostatic gating, geometric confinement, and heterojunction shape on hot electron transfer and by electron–electron scattering rates that can be altered by varying the charge carrier concentration in the NW FETs.

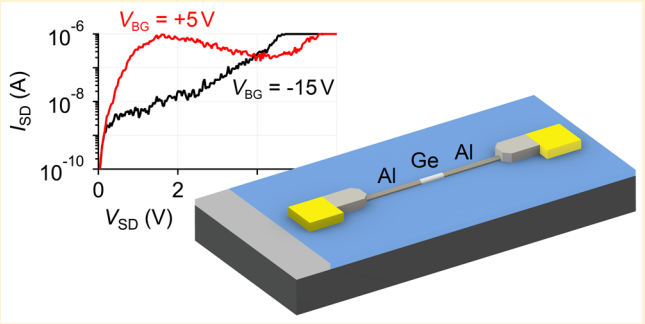

KEYWORDS: *nanowire, heterostructure, negative differential resistance, impact ionization, gate-tunable, germanium*

The success of continual miniaturization of electronic devices critically depends on the adoption of novel design paradigms enabling higher integration densities, lower power dissipation, and an overall improved performance. Low dimensional nanostructures, such as semiconductor NWs, present a promising approach for fabricating devices that can meet these requirements and could set new precedents. Thus, NWs have been the subject of extensive exploration into their remarkable potential for a range of novel device applications including tunnel FETs,[1,2] impact ionization FETs,[3] and single-electron devices,[4] to name but a few.

In some nanoscale systems, the astounding phenomenon of NDR has been observed.[5,6] This nonlinear electron transport phenomenon may enable fast switching logic circuits, static memory cells, or high-frequency oscillators.[7−9] Although several groups reported NDR in semiconductors at cryogenic temperatures,[10,11] it is rarely observed at room temperature except for the well-known Gunn effect in GaAs.[12] With regard to the above-mentioned future technological applications, it would be highly desirable to obtain NDR in complementary metal-oxide-semiconductor compatible materials at standard conditions and to control the effect by an electric field. Particularly, n-type Ge has been the subject of numerous studies in this regard because NDR is much more readily observed for electrons than for holes.[13] Electric fields oriented along the ⟨111⟩ axis in Ge have proven to show stronger signs of NDR than others due to their influence on electron populations in different subband valleys.[13,14] Thus, Al–Ge–Al NW heterostructures as shown in Figure 1 with ⟨111⟩ crystal orientation and abrupt metal–semiconductor heterointerfaces[15] represent an ideal model system for a detailed study of NDR in a geometrically confined system. The sophisticated device processing scheme[15] enables control of the active device length L_{Ge} and integration in electrostatically controlled FET device architecture. The Al–Ge–Al NW heterostructure resembles an equivalent circuit of two back-to-back Schottky diodes in series with the NW resistance. The abruptness of the Al–Ge Schottky contact is shown in the transmission electron microscopy image of the Al–Ge phase boundary in the inset of Figure 1a. The possibility to realize ultrashort Ge segments is used to ensure high electric fields along the ⟨111⟩ NW growth direction, realizing a configuration that has previously been shown to be most promising for observing NDR even at room temperature.[13]

The intrinsic, vapor–liquid–solid grown Ge NWs with diameters ranging from 30 to 40 nm were dispersed onto a highly p-doped Si substrate with a 100 nm thick, thermally grown SiO_2 layer and predefined macroscopic Ti–Au bonding pads (see Figure 1b). Individual NWs were then contacted with 100 nm thick Al pads by electron beam lithography, Al sputter deposition preceded by a HI dip, and lift-off techniques. To allow for electrostatic control of the charge carrier concentration within the intrinsic Ge NWs, the Si substrate was contacted by an additional Al pad to complete a NW FET in back-gated configuration. Subsequently, axial Al segments were formed in the NWs by thermal annealing for 300 s at 623 K in a

Received: August 10, 2015
Revised: September 24, 2015
Published: October 1, 2015

DOI: 10.1021/acs.nanolett.5b03169
Nano Lett. 2015, 15, 7514–7518

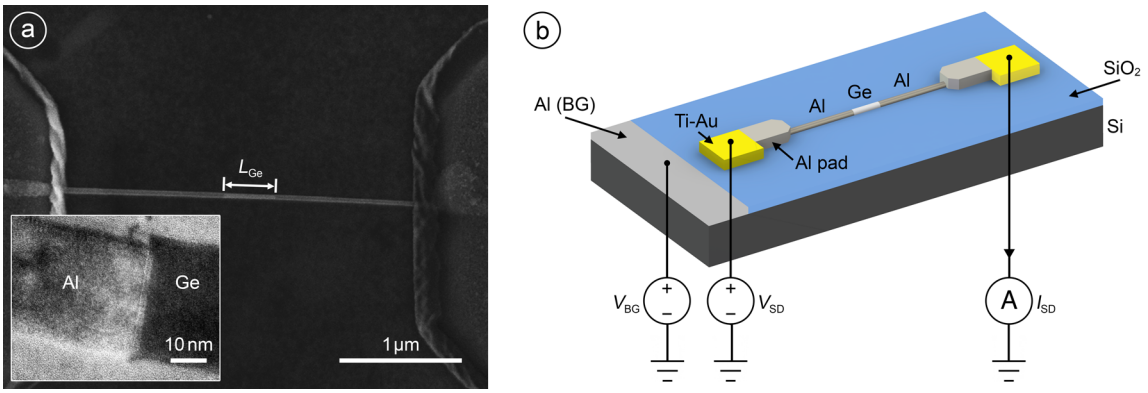

Figure 1. (a) SEM image of an Al−Ge−Al NW heterostructure with a Ge segment length of L_{Ge} = 415 nm. Inset: Transmission electron microscopy image of the abrupt Al−Ge interface. (b) Schematic illustration of the contacted Al−Ge−Al NW heterostructure resembling a back-gated NW FET with a 100 nm thick SiO_2 layer as gate dielectric and Al pads as the source/drain contacts, which are connected to larger Ti−Au bonding pads. An Al back-gate contact (Al BG) for biasing the substrate wafer is used to electrostatically control the charge carrier concentration in the Ge segment via a field effect.

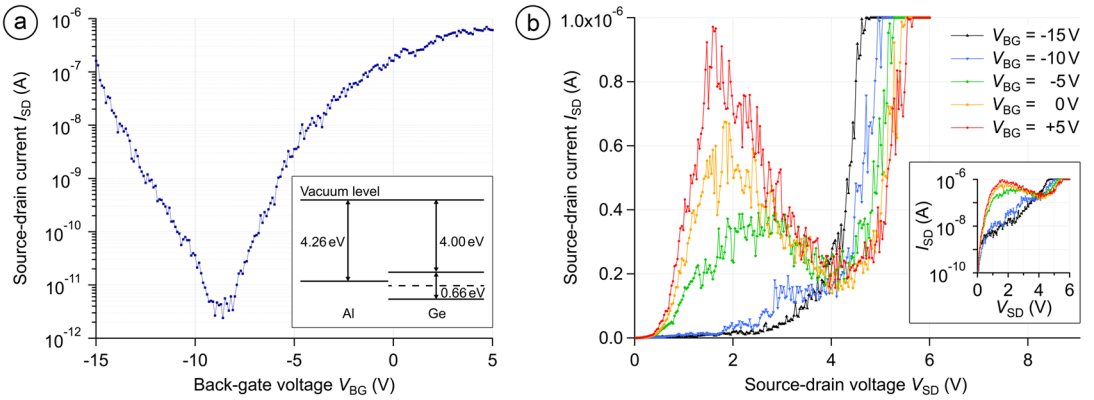

Figure 2. (a) Ambipolar transfer characteristic of a back-gated Al−Ge−Al NW heterostructure FET recorded at a source-drain voltage of V_{SD} = 1 V at standard conditions. Inset: Schematic energy level diagram of the Al−Ge system: The Fermi level of Al with a work function of 4.26 eV is close to midgap of Ge with an electron affinity of 4.00 eV and a band gap of 0.66 eV at 300 K. (b) $I-V$ plot displaying clear signatures of NDR and impact ionization for different back-gate voltages. Inset: Semilogarithmic representation of the $I-V$ measurement. A current compliance of 1 μA was in place to avoid melting induced failure due to Joule heating.

forming gas atmosphere.[15] Owing to the solubility of Ge in Al and the significantly different diffusion coefficients of Ge in Al and vice versa, a virtually complete substitution of Ge by Al occurs at the interface and a crystalline Al phase is formed along the NW.[15] The length L_{Ge} of the residual Ge segment is determined by the annealing time and temperature and the diameter of the NW. A scanning electron microscopy (SEM) image of an exemplary structure with a Ge segment length of L_{Ge} = 415 nm is shown in Figure 1a along with a schematic illustration of the fully featured back-gated NW FET (Figure 1b).

The transfer characteristic of the Al−Ge−Al NW heterostructure FET in Figure 2a exhibits ambipolar behavior with a maximum I_{ON}/I_{OFF} ratio of 10^4. Remarkably, high source-drain currents are achieved for both negative and positive back-gate voltages indicating effective charge carrier injection and accumulation of both electrons and holes in the NW channel. This can be understood in terms of the energy band alignment in the Al−Ge−Al NW heterostructure: The electron affinity of Ge of 4.00 eV and a band gap of 0.66 eV at 300 K[16] places the Fermi level of Al with a work function of 4.26 eV[17] close to midgap of Ge, as shown in the inset in Figure 2a. Therefore, for positive/negative back-gate voltages predominantly electrons/holes will accumulate in the channel and thus dominate the current transport. Previous observations have shown, that NDR is much more pronounced for electrons in comparison to holes,[8] which can be attributed to the small mobility differences achievable by the transfer of holes between subbands of the valence band.[13] Thus, the ambipolar transfer characteristics of the NW FETs are used to ensure a high concentration of electrons in the ⟨111⟩ oriented Ge NW segments, enabling NDR via intervalley electron transfer processes.

Electrical characterizations performed at room temperature and at ambient pressure revealed NDR as well as an onset of impact ionization at sufficiently high electric fields in the Ge segments of the Al−Ge−Al NW heterostructures. The main plot in Figure 2b shows the $I-V$ characteristic of an Al−Ge−Al NW heterostructure with a total length of 3.4 μm and an unreacted Ge segment with a length of 554 nm and a diameter of 35 nm for various back-gate voltages. The $I-V$ curves were recorded by linearly increasing the source-drain voltage while monitoring the source-drain current for different back-gate voltages. Above a certain threshold electric field, a sudden increase in source-drain current indicates the onset of impact ionization. A threshold electric field value of E_{th} = 76 kV cm^{-1} at a back-gate voltage of V_{BG} = −15 V was determined from the

DOI: 10.1021/acs.nanolett.5b03169
Nano Lett. 2015, 15, 7514−7518

zero-crossing of a linear fit of the steep increase in the $I-V$ curve, which is in good agreement with the previously reported impact ionization threshold electric field of Al−Ge−Al NW heterostructures of 80 kV cm^{-1}[15] and the breakdown electric field of bulk Ge of 100 kV cm^{-1}.[18] Increasingly positive back-gate voltages shift the onset of impact ionization to higher electric fields, due to the impact ionization rates for holes being higher than those for electrons in Ge.[19,20]

A clear signature of NDR is present for $V_{BG} > -10$ V and becomes even more apparent for positive back-gate voltages, as shown in Figure 2b. The magnitude of the current peak before the NDR region depends on the charge carrier concentration in the Ge segment of the NW and can be controlled by means of the applied back-gate voltage. For a back-gate voltage of V_{BG} = +5 V, remarkably high current densities of up to $J = 10^5$ A cm^{-2} were observed before NDR set in. As a quantitative measure of the magnitude of the NDR phenomenon, the PVR, that is the ratio of the maximum current I_{peak} before the NDR region and the current I_{valley} at the local minimum in the $I-V$ characteristic was extracted for different back-gate voltages. More positive back-gate voltages generally resulted in higher PVR values. At room temperature, a maximum PVR of 42 was achieved for a NW heterostructure with a Ge segment length of L_{Ge} = 544 nm, unambiguously allowing the identification of NDR in the $I-V$ plots and hinting at a high number of charge carriers participating in effects leading to this behavior. The measured PVR at 300 K is significantly higher than previously reported room temperature PVR values of 1.7 or 4.5 for Ge quantum dot tunneling diodes[21] or GaN NWs,[22] respectively. The influence of the back-gate voltage on the PVR and the onset electric field of NDR is a key advantage of the presented three-terminal devices and may be used for realizing oscillators with an electrostatically controllable output power.[9]

While impact ionization was observed for all Al−Ge−Al NW heterostructures, the occurrence of NDR appeared to be critically dependent on the fabrication process, particularly on the contact formation procedure. Al−Ge−Al NW heterostructures, which were processed rapidly to minimize reoxidation of the Ge NWs after the HI dip before Al sputter deposition were more likely to exhibit signatures of NDR. Additionally, moderate reverse sputtering prior to the Al deposition also increased the yield for samples exhibiting clearly identifiable NDR. These samples show distinct ambipolar transfer characteristics, which appeared to be a reliable indication of the occurrence of NDR in the NW heterostructures.

According to Kazazis et al.,[8] one has to consider self-heating effects, charge carrier trapping, and the transferred electron effect as potential origins of NDR. Additionally, for nanostructures, NDR may also be induced by resonant tunneling between quantized energy levels, as was reported for GaN/AlN double-barrier heterostructure NWs.[23] However, no such resonance effects can be considered for the actual device architecture and the opposite gate dependency of the NDR current peak leads us to exclude this mechanism for the studied devices.

In bipolar transistors with heavily doped bases, larger collector-emitter voltages and collector currents may elevate the junction temperature and result in a decrease of the current gain, which is determined by the base recombination current of the devices.[24] Therefore, in a certain region, an increase in voltage leads to a decrease in current due to local heating. This effect can be excluded for the presented Al−Ge−Al NW device, as for this unipolar device heating would increase the number of charge carriers and thus the overall conductivity. Furthermore, self-heating has also been reported to induce NDR in SOI based transistors. For these thin materials, NDR is attributed to charge carrier mobility degradation due to local heating as a result of power dissipation in the transistor channels.[25−27] NDR due to self-heating in SOI transistors is significantly more pronounced in devices with shorter channels as a result of a higher drive current and less semiconductor volume.[25] For the Al−Ge−Al NW heterostructures, clear and strong signatures of NDR were observed in back-gated FETs with channel lengths ranging from 144 nm to 2.55 μm. For all these devices, NDR was induced by increasing the electric field above a certain threshold. Thus, for longer devices the occurrence of NDR shifted to higher V_{SD} values but appeared to be independent of the total current. The wide range of Ge segment lengths, which displayed similarly pronounced NDR, leads us to the conclusion that the observed NDR is not caused by charge carrier mobility degradation due to self-heating. Additionally, temperature dependent measurements revealed that higher temperatures resulted in increased absolute currents. Therefore, local heating in the presented NW heterostructures cannot induce NDR.

The trapping of charge carriers at interface states may also lead to NDR.[8] At sufficiently high energies, charge carriers may get trapped in surface/interface traps that contribute to additional surface scattering, effectively lowering carrier mobility, and gate coupling. The contribution of charge carrier trapping to the observed NDR can be readily distinguished by performing loop measurements.[8] Such loop measurements performed on the Al−Ge−Al NW heterostructures displayed clear signatures of NDR (see Supporting Information), leading to the conclusion that the transferred electron effect is the predominant origin of the NDR phenomenon in the studied NW heterostructure devices.

At sufficiently high electric fields, electrons from an energetically favorable conduction band valley characterized by a low effective mass and thus high mobility can be scattered to a heavy mass valley with lower mobility increasing the resistivity of the material and manifesting itself in NDR.[28] This so-called transferred electron effect has been observed in numerous systems including GaAs,[29] GaN nanocrystals,[30] and Ni/Ge Schottky diodes.[28] According to the Ridley−Watkins−Hilsum theory,[31] a semiconductor must fulfill three requirements to achieve NDR by the transferred electron effect: (i) the lower and upper valleys between which electrons are transferred must be separated by an energy difference much larger than the thermal energy, (ii) the separation of said energy levels must be smaller than the energy gap of the semiconductor, (iii) electrons in the lower valley must have higher mobility (lower effective mass) than those in the upper valley.[29] The first two conditions are met for Ge by the L-point and Δ-point minima of the ⟨111⟩ and ⟨100⟩ subbands of the conduction band, respectively, as shown in Figure 3.

The energy difference between the L-point and Δ-point minima of Ge is ΔE = 0.19 eV,[32] which is significantly higher than the thermal energy at T_{RT} = 300 K, that is, $k_B T_{RT}$ = 25.8 meV (with Boltzmann constant k_B). However, the latter condition appears to be inhibiting the occurrence of NDR due to electron transfer. This holds true for the longitudinal effective electron masses; however, the transverse effective electron mass in the Δ-point minimum, $m^*_{\Delta,t} = 0.288\ m_0$, is significantly higher than that in the L-point minimum, $m^*_{L,t}$ =

DOI: 10.1021/acs.nanolett.5b03169
Nano Lett. 2015, 15, 7514−7518

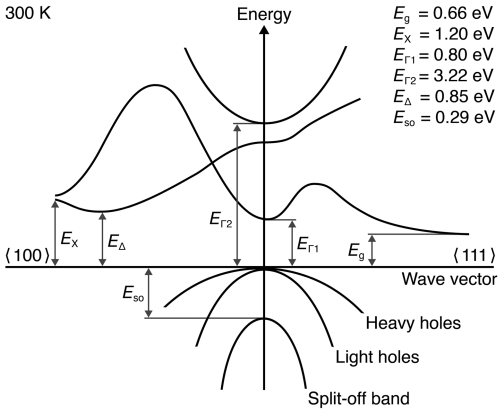

Figure 3. Schematic diagram of the energy band structure of Ge. The conduction band edge occurs at the hexagonal face centers, while the valence band edge occurs at the central zone point. The width of the forbidden band is 0.66 eV at room temperature. The spin−orbit splitting at the valence band edge is approximately 0.29 eV. The lowest conduction band has three types of minima: four 111 minima (at the band edge), one 000 minimum, and six 100 minima. The 000 minimum lies 0.14 eV above the 111 minima; the 100 minima lie 0.19 eV above the 111 minima. Image adapted from ref 32.

0.082 m_0 (with the free electron mass m_0),[11] permitting the NDR phenomenon to occur. Additionally, Monte Carlo simulations have shown, that band nonparabolicity and the presence of upper valleys both contribute to a reduced electron mobility, with a stronger contribution of the latter.[11] Although the Γ-point minimum is energetically closer to the L-point minimum, the coupling constant between 111 and 000 minima is significantly lower than between 111 and 100 minima.[11] Thus, the transfer of electrons mainly occurs from the L-point minimum to the Δ-point minimum. The energy difference of ΔE = 0.19 eV[32] between the favorable L-point minimum and the energetically higher Δ-point minimum determines the threshold electric field for electron repopulation. As shown in Figure 2b, the onset of NDR is shifted to lower electric fields for higher back-gate voltages, that is, increased electron concentrations. This can be understood in terms of the energetically highest states occupied by electrons in the lowest conduction band valley: In the case of a high electron concentration, higher states in the L-point minimum need to be occupied to accommodate all electrons in the system. Because electrons in these states are already at a higher energy level they need to overcome a smaller energy difference to be scattered to higher valleys like the Δ-point minimum. Therefore, smaller electric fields are required to activate electron transfer processes and the position of the current peak is shifted toward lower electric fields for more positive back-gate voltages, realizing an electrostatic control mechanism for the onset electric field of NDR.

The transfer of electrons between conduction band valleys with significantly different effective electron masses also accounts for the increased impact ionization threshold electric fields at more positive back-gate voltages, that is, higher electron concentrations, because electrons in low mobility valleys are not accelerated by an electric field as efficiently as electrons in a high mobility valley. At high electron concentrations, transfer to energetically higher conduction band valleys with lower electron mobilities sets in at lower electric fields leading to a high number of electrons in these valleys. Therefore, higher electric fields are required for avalanche breakdown in the case of more positive back-gate voltages, that is, higher electron concentrations.

The dynamic of electron transport phenomena in the NW heterostructures was also studied at different temperatures ranging from 100 K up to room temperature at a pressure of 10^{-4} mbar. The $I-V$ plot of an Al−Ge−Al NW heterostructure with a Ge segment length of L_{Ge} = 487 nm recorded at a constant back-gate voltage of V_{BG} = +15 V for different temperatures is shown in Figure 4. The magnitude of the NDR

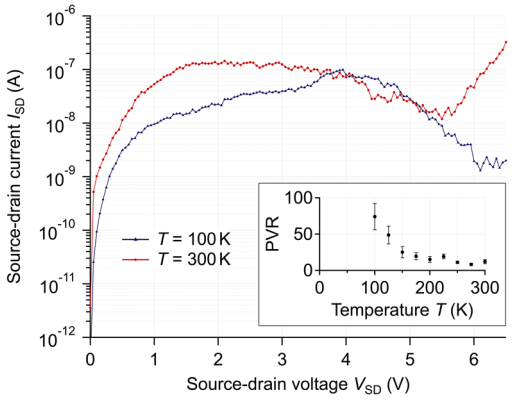

Figure 4. $I-V$ measurements taken at different temperatures at a constant back-gate voltage of V_{BG} = +15 V show more pronounced NDR at lower temperatures. The inset shows an increase of the calculated PVR from 12 ± 3 at room temperature to 74 ± 18 at 100 K.

signature increases significantly with decreasing temperature. The PVR at different temperatures ranging from 100 to 300 K is shown in the inset in Figure 4. A maximum PVR of 74 ± 18 was measured for the lowest temperature. As a result of decreased thermal excitations and a higher fraction of electrons in the low energy states of the high mobility subband valley, the current peak before the NDR region is shifted to higher electric fields for lower temperatures. The initially lower average energy of the electrons at decreased temperatures also leads to a shift of the onset of impact ionization to higher electric fields.

In conclusion, more than ten ambipolar Al−Ge−Al NW FETs exhibited both NDR and impact ionization at room temperature. By modulating the charge carrier concentration in the Ge segments through electrostatic fields, that is, back-gate voltages, the occurrence of NDR and the threshold electric fields for NDR and impact ionization were controlled. While self-heating and charge carrier trapping could be excluded as the primary causes of the observed behavior, the observation of NDR in the NW heterostructures is attributed to the transferred electron effect. Charge carrier confinement in the quasi-one-dimensional NWs leads to an unprecedented maximum PVR of 42 at room temperature. At lower temperatures, the magnitude of the PVR of the NDR region was shown to be higher, whereas the transfer phenomenon remained clearly identifiable even at 300 K. The fabricated three-terminal devices could prove to be of great technological interest for operating future devices combining NDR and impact ionization with conventional FET technology at standard conditions.

DOI: 10.1021/acs.nanolett.5b03169
Nano Lett. 2015, 15, 7514−7518

■ ASSOCIATED CONTENT

Supporting Information

The Supporting Information is available free of charge on the ACS Publications website at DOI: 10.1021/acs.nanolett.5b03169.

Loop measurement of NDR and calculation of charge carrier concentration in Ge NW segment as a function of the back-gate voltage. (PDF)

■ AUTHOR INFORMATION

Corresponding Author

*E-mail: alois.lugstein@tuwien.ac.at.

Author Contributions

The manuscript was written through contributions of all authors. All authors have given approval to the final version of the manuscript.

Notes

The authors declare no competing financial interest.

■ ACKNOWLEDGMENTS

The authors gratefully acknowledge financial support by the Austrian Science Fund (FWF): project No. I 841-N24 and I 724-N16 and technical support by USTEM TU Wien. The authors further thank the Center for Micro- and Nanostructures (ZMNS) for providing the cleanroom facilities and Hermann Detz (ZMNS) for the support with low temperature measurements.

■ REFERENCES

(1) Tomioka, K.; Fukui, T. *Appl. Phys. Lett.* **2011**, *98* (8), 083114.
(2) Moselund, K. E.; Ghoneim, H.; Björk, M. T.; Schmid, H.; Karg, S.; Lörtscher, E.; Riess, W.; Riel, H. *Device Res. Conf. - Conf. Dig. DRC* **2009**, *52* (8), 23−24.
(3) Bjork, M. T.; Hayden, O.; Knoch, J.; Riel, H.; Schmid, H.; Riess, W. In *65th Annual Device Research Conference*; Institute of Electrical and Electronics Engineers (IEEE): Piscataway, NJ, 2007.
(4) Thelander, C.; Mårtensson, T.; Björk, M. T.; Ohlsson, B. J.; Larsson, M. W.; Wallenberg, L. R.; Samuelson, L. *Appl. Phys. Lett.* **2003**, *83* (10), 2052.
(5) Shih, A.; Fathololoumi, S.; Zhao, S.; Huy, B. Le; Pham Trung Nguyen, H.; Shih, I.; Mi, Z. *Int. J. Theor. Appl. Nanotechnol.* **2014**, *1* (1), 105−110.
(6) Rinkiö, M.; Johansson, A.; Kotimäki, V.; Törmä, P. *ACS Nano* **2010**, *4* (6), 3356−3362.
(7) Hong, I.-H.; Chen, T.-M.; Tsai, Y.-F. *Appl. Phys. Lett.* **2012**, *101*, 053113.
(8) Kazazis, D.; Zaslavsky, A.; Tutuc, E.; Bojarczuk, N. A.; Guha, S. *Semicond. Sci. Technol.* **2007**, *22* (1), S1−S4.
(9) Wu, Y.; Farmer, D. B.; Zhu, W.; Han, S.-J.; Dimitrakopoulos, C. D.; Bol, A. A.; Avouris, P.; Lin, Y.-M. *ACS Nano* **2012**, *6* (3), 2610−2616.
(10) Elliott, B. J.; Gunn, J. B.; McGroddy, J. C. *Appl. Phys. Lett.* **1967**, *11* (8), 253−255.
(11) Jacoboni, C.; Nava, F.; Canali, C.; Ottaviani, G. *Phys. Rev. B: Condens. Matter Mater. Phys.* **1981**, *24* (2), 1014−1026.
(12) Gunn, J. B.; Elliott, B. J. *Phys. Lett.* **1966**, *22* (4), 369−371.
(13) Smith, J. E.; McGroddy, J. C.; Nathan, M. I. *Phys. Rev.* **1969**, *186* (3), 727−734.
(14) Fawcett, W. *Electron. Lett.* **1967**, *3* (11).
(15) Kral, S.; Zeiner, C.; Stöger-Pollach, M.; Bertagnolli, E.; den Hertog, M. I.; Lopez-Haro, M.; Robin, E.; El Hajraoui, K.; Lugstein, A. *Nano Lett.* **2015**, *15* (7), 4783−4787.
(16) Kasap, S.; Capper, P. *Springer Handbook of Electronic and Photonic Materials*; Springer Science and Business Media: New York, 2006; Vol. *10*.
(17) Eastment, R. M.; Mee, C. H. B. *J. Phys. F: Met. Phys.* **1973**, *3* (9), 1738−1745.
(18) Levinshtein, M.; Rumyantsev, S.; Shur, M. *Handbook Series on Semiconductor Parameters*; World Scientific: Singapore, 1996.
(19) Miller, S. L. *Phys. Rev.* **1955**, *99* (4), 1234−1241.
(20) Yeom, K.; Hinckley, J.; Singh, J. *J. Appl. Phys.* **1996**, *80*, 6773−6782.
(21) Oehme, M.; Karmous, A.; Sarlija, M.; Werner, J.; Kasper, E.; Schulze, J. *Appl. Phys. Lett.* **2010**, *97* (1), 012101.
(22) Dhabal, A.; Chander, D. S.; Ramkumar, J.; Dhamodaran, S. *Micro Nano Lett.* **2011**, *6* (4), 280.
(23) Songmuang, R.; Katsaros, G.; Monroy, E.; Spathis, P.; Bougerol, C.; Mongillo, M.; De Franceschi, S. *Nano Lett.* **2010**, *10* (9), 3545−3550.
(24) Wan-rong, Z.; Lian-cang, Z.; Jing-wei, Y.; Hai-jiang, L.; Yan, H.; Feng-ying, G.; Li-ming, L.; Zhe, W.; Jian-jun, Q.; Pan, G. *Proc. 7th Int. Conf. Solid-State Integr. Circuits Technol.* **2004**, *3*, 2155−2158.
(25) McDaid, L. J.; Hall, S.; Mellor, P. H.; Eccleston, W.; Alderman, J. C. *Electron. Lett.* **1989**, *25*, 827.
(26) Jomaah, J.; Balestra, F.; Ghibaudo, G. *Proc. 1993 IEEE Int. SOI Conf.* **1993**, 82−83.
(27) Eng, Y.-C.; Lin, J.-T.; Lin, P.-H.; Huang, H.-Y.; Kang, S.-S.; Kao, K.-K.; Lin, J.-D.; Tseng, Y.-M.; Tsai, Y.-C. *2008 26th International Conference on Microelectronics* **2008**, 485−488.
(28) Husain, M. K.; Li, X. V.; De Groot, C. H. *IEEE Electron Device Lett.* **2009**, *30* (9), 966−968.
(29) Vlaardingerbroek, M. T. *1st Eur. Microw. Conf.* **1969**, 206.
(30) Chitara, B.; Ivan Jebakumar, D. S.; Rao, C. N. R.; Krupanidhi, S. B. *Nanotechnology* **2009**, *20* (40), 405205.
(31) Ridley, B. K.; Watkins, T. B. *Proc. Phys. Soc., London* **1961**, *78* (2), 293−304.
(32) Ge−Germanium Band structure and carrier concentration. http://www.ioffe.ru/SVA/NSM/Semicond/Ge/bandstr.html (accessed Sept 23, 2015).

DOI: 10.1021/acs.nanolett.5b03169
Nano Lett. 2015, 15, 7514−7518